Modelling of ethylene polymerization with Cp_2ZrCl_2/MAO catalyst

J. M. Vela Estrada and A. E. Hamielec*
Institute for Polymer Production Technology, Department of Chemical Engineering, McMaster University, Hamilton, Ontario L8S 4L7, Canada
(Received 15 April 1992; revised 2 July 1993)

A full, two-level factorial experimental design with temperature and concentrations of zirconocene dichloride and methylaluminoxane as variables was employed to study the polymerization of ethylene. Rate of polymerization and molecular weight data were used to develop a kinetic model and estimate the kinetic parameters. The polymerization rate was continuously recorded from a semi-batch reactor and molecular weights were measured at the end of each experimental run. The analysis of the data suggests the presence of two kinds of active species. One kind of species is produced from the other via a pseudo-first-order reaction.

(Keywords: zirconocene; methylaluminoxane; polyethylene)

INTRODUCTION

Commercially, high density polyethylene is produced using heterogeneous Ziegler–Natta catalysts of titanium or chromium compounds. The productivity of these catalysts has been significantly improved and typically they produce polyethylene with broad molecular weight distributions ($M_w/M_n = 4$–24)[1]. On the other hand, soluble Ziegler–Natta catalysts based on zirconium have been reported to be much more active than some heterogeneous catalysts[2,3] and they produce polymers with narrow molecular weight distributions (*MWDs*) ($M_w/M_n = 2$–5)[2,4,5]. Therefore, soluble catalysts can produce new products (narrow *MWD*, high density polyethylene) without the need for eliminating catalyst residues from the polymer.

Even though the high activity of soluble catalysts is very encouraging for commercial applications, the kinetics of this catalyst system have not been studied extensively.

Kaminsky *et al.*[4,6] reported that by varying the concentration of Cp_2ZrCl_2 and temperature they were able to regulate molecular weight, and also reported that the lifetime of the catalyst is remarkably long. Schmidt[7] also reported a large variation of the molecular weight with polymerization temperature. He attributed the effect of catalyst concentration on molecular weight to the change in molar ratio of cocatalyst to catalyst.

Chien and Wang[8] proposed the first and still the only kinetic model for the polymerization of ethylene using the zirconocene dichloride (Cp_2ZrCl_2) catalyst system. The model assumes the presence of multiple active centre types, chain transfer to methylaluminoxane (MAO), chain transfer to hydrogen, β-hydride chain transfer, one first-order deactivation reaction at 0°C and two first-order deactivation reactions at higher temperatures. The average propagation rate constant for the various site types was estimated from productivity data and the experimentally determined number of active sites. The β-hydride chain transfer rate constant and the transfer to hydrogen rate constant were estimated using number average molecular weight data. The transfer to aluminium rate constant was estimated from metal–polymer bond concentration data, and the deactivation rate constants were estimated from polymerization rate data. Unfortunately, they did not make a comparison between experimental and predicted polymerization rates and number average molecular weights, nor did they show the precision of each estimate.

In this study a semi-batch reactor was used for ethylene polymerization. Experiments were carried out at preselected operating conditions according to a full, two-level factorial design. The polymerization rate was measured continuously as a function of time and molecular weights were determined at the end of each run to provide data for kinetic model development and parameter estimation. The effects of the operating variables, i.e. temperature and concentrations of Cp_2ZrCl_2 and MAO, on those parameters were analysed using empirical relationships. The model includes the presence of two active site types with the gradual transition of one site type to the other. The model-calculated average molecular weights and polydispersities (2 and higher) agree with the experimental data very well. The acceleration in polymerization rate from a value reached within the first three minutes of reaction time was also predicted by this model.

EXPERIMENTAL PROCEDURE

Materials and synthesis procedure

The semi-batch reactor used in this study is shown in *Figure 1* (1000 ml stainless steel kettle with a continuous feed of ethylene at constant pressure). It was equipped with a magnetic stirring drive and the necessary reactant inlets. Temperature was controlled by regulating the

* To whom correspondence should be addressed

0032-3861/94/04/0808–11

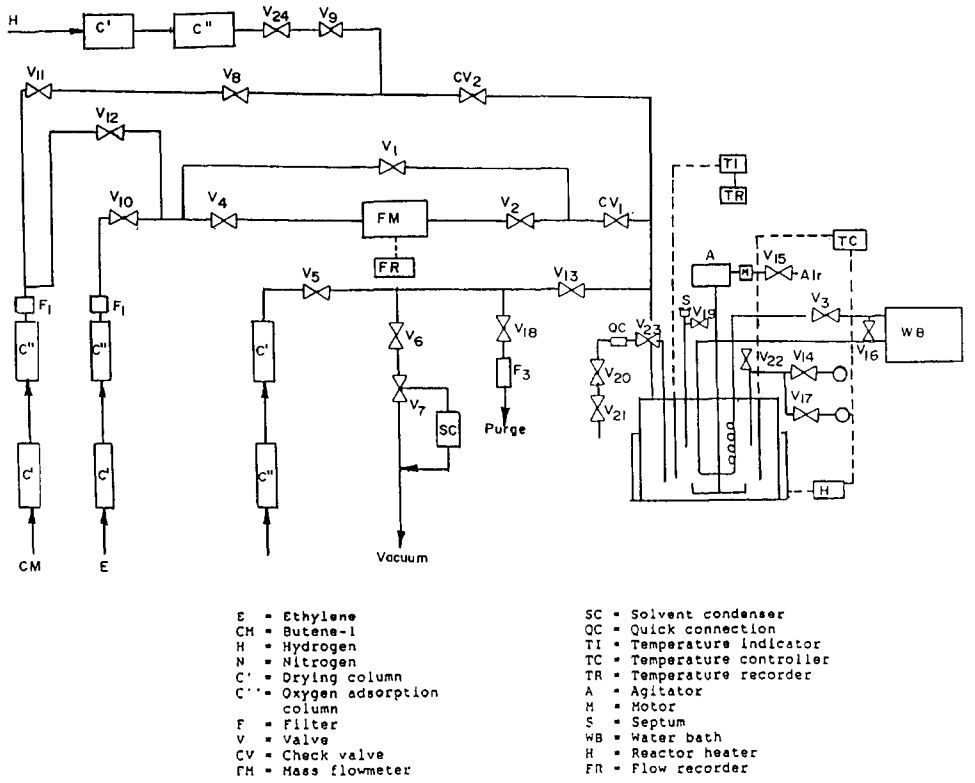

Figure 1 Diagram of the polymerization system

power of an electrical jacket heater and manually adjusting the cold water flow through a coil inside the reactor. The temperature could be easily maintained to within 1°C from the target value.

The ethylene monomer, research grade with a purity of 99.98%, was obtained from Matheson. Ethylene was passed through a drying column containing type 3A molecular sieves. High purity nitrogen (99.99%) was dried with a drierite column. Aldrich Chemical Co. provided Cp_2ZrCl_2 (98% pure), a 25 wt% solution of trimethylaluminium (TMA) in toluene and 98% pure aluminium sulfate octadecahydrate. The certified ACS analytical reagent grade toluene was dried by refluxing under a nitrogen atmosphere with sodium metal for at least two days.

In the synthesis of MAO, the procedure patented by Kaminsky and Hahnsen[9] was followed using a glove box. A safe MAO synthesis was carried out at 25°C by combining the solution of TMA with hydrated aluminium sulfate in a batch reactor with a continuous flow of dry nitrogen through the glove box. The solution was separated from the solid aluminium sulfate by filtration and was then employed as a master batch. Two MAO batches of concentrations 1.325 (batch 1) and 1.318 mol l^{-1} (batch 2) were prepared and no characterization such as molecular weight measurement of the synthesized MAO was performed.

In the synthesis of high density polyethylene, the reactor was assembled and flushed with dry nitrogen several times. Dry toluene was then added followed by nitrogen and ethylene, in that order, until a total pressure of 20 psi (1 psi = 6895 Pa) was reached. The partial pressure of ethylene and the stirring speed were 10 psi and 1500 rev min^{-1}, respectively, in every run. It was found that at this stirring speed the effect of monomer diffusion on polymerization was negligible (polymerization was reaction controlled). MAO was then added followed by a solution of zirconocene dichloride in toluene. A master batch of this solution had been previously prepared.

The ethylene polymerization rate in cm^3 min^{-1} at 25°C and 1 atm (sccm) was continuously recorded for an hour on a strip chart recorder using a mass flowmeter. Later, the units of the rate data were converted to mol min^{-1} for the parameter estimation. The polymer yield estimated from the consumption rate of ethylene agreed to within 6.9% with that measured by the weighing of the polymer produced after polymerization was complete. High temperature gel permeation chromatography (g.p.c.) (Waters 150-C) with a differential refractive index detector was used for the determination of M_n and M_w. The g.p.c. chromatograms were recorded at 140°C using trichlorobenzene as solvent.

Experimental design strategy

As mentioned earlier, a full, two-level factorial design guided the selection of the operating conditions. The conditions used for the experimental runs are shown in *Table 1*. The same batch of synthesized MAO was employed for all the runs except for one set of operating conditions (R-15-R1, R-15-R2 and R-15-R4). As will be discussed later, the molecular weight distribution of the polymer is very sensitive to the MAO synthesis conditions.

Repeated runs were performed at selected operating conditions, and they are denoted by a suffix -R1, -R2, -R3, etc. The best replicates were chosen to estimate the pure error variance of the polymerization rate data between runs and within runs and the pure error variance of the molecular weight data. These error variance

Table 1 Operating conditions for polymerization experiments[a]

Run	Replicates	$[Al]_0$ (mmol l^{-1})	$[Zr]_0$ (mmol l^{-1})	T (°C)	MAO batch
R-24	R2	21.08	13.08×10^{-3}	71	2
R-18	R1	21.08	13.08×10^{-3}	50	2
R-22	R1	21.08	6.54×10^{-3}	71	2
R-19	R1	21.08	6.54×10^{-3}	50	2
R-23	R1	13.8	13.08×10^{-3}	71	2
R-20	R1	13.18	13.08×10^{-3}	50	2
R-21	R1	13.18	6.54×10^{-3}	71	2
R-17	R2, R3	13.18	6.54×10^{-3}	50	2
R-15	R1, R2, R4	13.18	6.54×10^{-3}	50	1

[a] Initial reaction volume measured at 25°C was 600 ml

estimates are required to examine the reproducibility of the molecular weight data, to assess the adequacy of the fitted rate model, and to evaluate the precision of the estimated model parameters. The chain transfer rate constants of the molecular weight models can be estimated, but evaluation of their precision is not possible since only the molecular weight of the final product was measured.

The selection of the best replicates to estimate the pure error variance makes the test for model adequacy more sensitive. However, the selected replicates included runs in which dried solvent from different batches was employed, and, as a result of that, the estimated variance includes this source of experimental variation.

EXPERIMENTAL RESULTS

Data interpretation

Rate data. *Figure 2* shows the polymerization rate data at 50°C with $[Al]_0$ at 21.08 mmol l^{-1}, $[Zr]_0$ at 13.08×10^{-3} mmol l^{-1} and using the MAO prepared in batch 2. For the second run, all of the synthesis conditions were the same as for the first run except that $[Zr]_0$ was lowered to 6.54×10^{-3} mmol l^{-1}. Complete details for these runs (R-18-R1 and R-19-R1) may be found in *Table 1*. The rates of monomer consumption near time zero exhibit a rapid increase. These rates appear to reach primary maxima which last for a few minutes and then rapidly reach secondary maxima, whereupon slow decreases in rate, which last for about 60 min (the maximum time for the run), are observed. This rate acceleration period (time to reach the secondary maximum) is longer for runs using lower levels of zirconium. As will be shown later, runs done at 71°C do not have a rate acceleration period nor do they show any decrease in polymerization rate over the run time (a 1 h period).

Figure 3 shows additional polymerization rate data at 50°C for different batches of MAO. Rate measurements for batch 1 (MAO) were repeated three times and for batch 2 (MAO) twice. Except for one run (R-15-R1), in which a different solvent (toluene) batch was used, the reproducibility is excellent with the rate acceleration period reproduced well for both MAO batches at the 50°C polymerization temperature. This reproducibility and the sensitivity of the induction period to the polymerization conditions strongly suggest that a rate acceleration period is an inherent property of this system at 50°C.

It appears that such a rate acceleration period has not been reported for this catalyst system. Kaminsky[5], Kaminsky and Schlobohm[6] and Chien and Wang[2,8] did not report seeing such an induction period. It is likely that the reason why these authors did not see this rate acceleration period was that their polymerization temperatures (60–90°C) were higher than 50°C.

Reichert[10] reported a similar rate acceleration period for ethylene polymerization at 10°C but with a different catalyst system, namely $Cp_2TiEtCl/AlEtCl_2$. Reichert's explanation was as follows. He suggested that during the rate acceleration period the polymerization is homogeneous, and shortly before the secondary maximum occurs the polymerization becomes heterogeneous. Precipitated polyethylene in his reactor led him to believe that the secondary maximum was due to a temperature increase within the polymer particles, or to an increase in concentration of reactants (active sites and ethylene monomer). Assuming the presence of only one site type, the model given by Reichert would fail to explain the significant deactivation of active sites at 50°C indicated by the polymerization rate data shown in *Figure 4*. The catalyst deactivates significantly at 50°C, but hardly at all at 71°C. A higher deactivation rate at a lower temperature for a catalyst with a single site type is strange behaviour indeed.

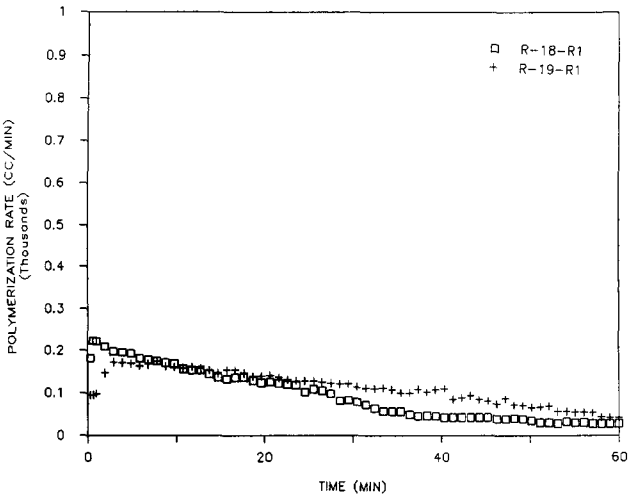

Figure 2 Kinetic rate curves showing the different induction periods for $[Zr]_0 = 13.08 \times 10^{-3}$ mmol l^{-1} (R-18) and $[Zr]_0 = 6.54 \times 10^{-3}$ mmol l^{-1} (R-19). $[Al]_0 = 21.08$ mmol l^{-1} and $T = 50$°C

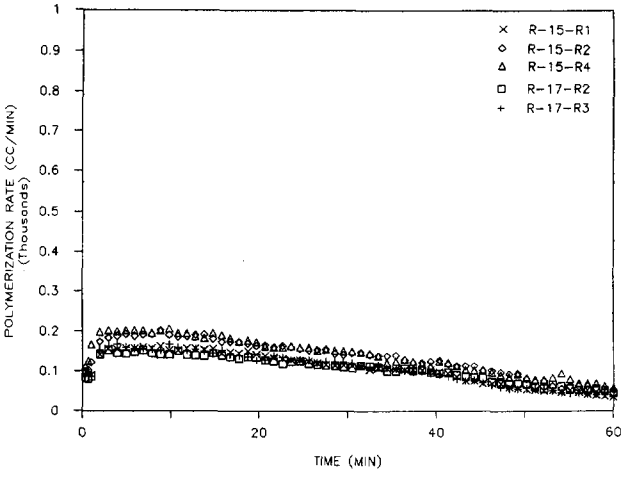

Figure 3 Polymerization runs using different MAO batches (MAO batch 1, R-15; MAO batch 2, R-17). $[Zr]_0 = 6.54 \times 10^{-3}$ mmol l^{-1}, $[Al]_0 = 13.18$ mmol l^{-1} and $T = 50$°C

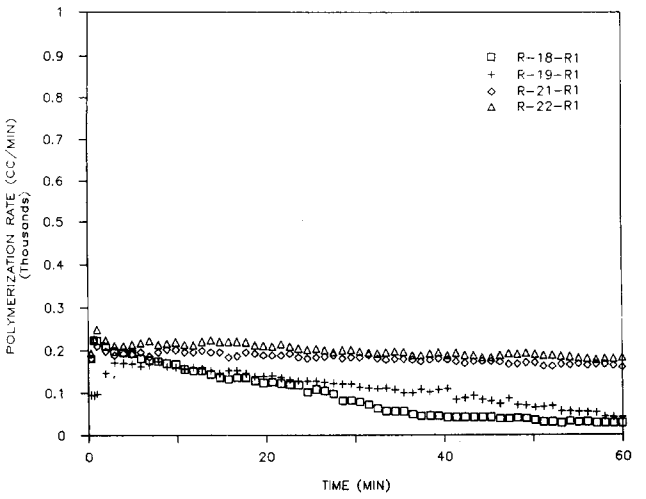

Figure 4 Kinetic rate curves showing the different catalyst decay rates with MAO batch 2 at $T = 50°C$ (R-18, R-19) and 71°C (R-21, R-22). The operating conditions for $[Zr]_0$ and $[Al]_0$ can be found in *Table 1*

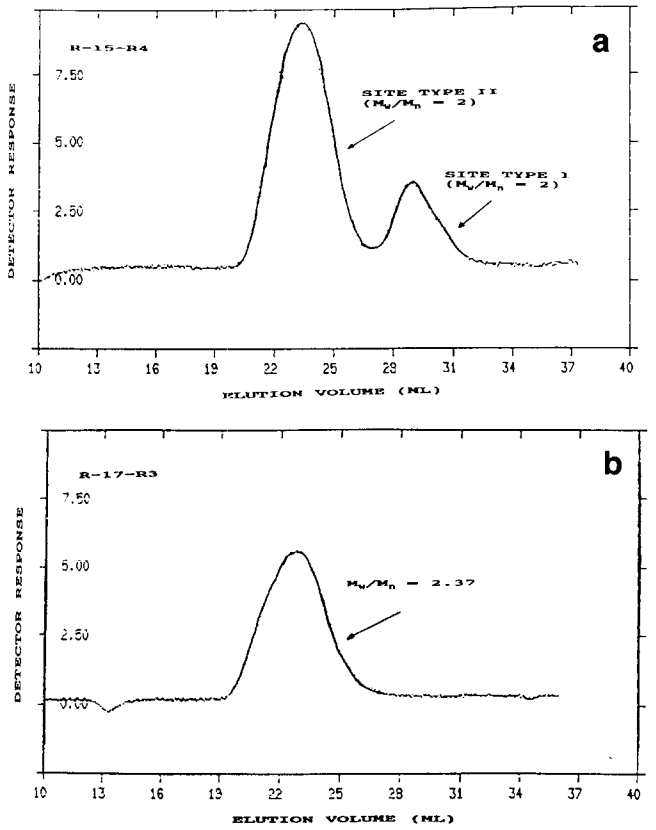

Figure 5 *MWDs* of polymer samples synthesized at 50°C with different MAO batches: (a) batch 1; (b) batch 2

Molecular weight data. *Figure 5* shows g.p.c. detector responses for two different runs using MAO batches 1 and 2. The response for MAO batch 1 indicates a bimodal distribution. Integration of the two peaks separately to calculate number average and weight average molecular weights gives a polydispersity of 2 for each peak. This strongly suggests that there are two catalyst site types present with each site type producing one of the peaks. Hence in *Figure 5* for run R-15-R4, the peaks are labelled as polymer products produced by site type I and site type II. Site type I produces lower molecular weight polyethylene and hence has a higher chain transfer/propagation rate constant ratio. A comparison of the areas under the detector responses indicates that site type II has produced more polyethylene than site type I at 50°C. The g.p.c. response for polyethylene produced in run R-17-R3 is unimodal and the polydispersity is 2.37, suggesting that the ratios of chain transfer/propagation rate constant for site type I and site type II differ more for MAO batch 1 than for MAO batch 2. This difference is likely due to the chain transfer rate constants of the two site types rather than to their propagation rate constants. The reproducibility and similarity of the rate data for the two MAO batches shown in *Figure 4* suggest that the propagation rate constants for the two site types produced with MAO batch 1 are close to the propagation rate constants for the two site types produced with MAO batch 2.

Table 2 gives the molecular weight averages measured for all of the runs in this study. The polydispersities of the polymers produced at 71°C (runs R-21, R-22, R-23, and R-24) are 2.05, 1.96, 1.97, and 1.97. All of these polydispersities are equal to 2 within experimental error, and one can therefore conclude that at 71°C there is only one site type producing polyethylene and that chain transfer reactions play a dominant role in producing the polymer. The polymer produced at 50°C is unimodal or bimodal and the polydispersities of the whole polymer samples are significantly greater than 2. For example, the polydispersities of the unimodal samples are 3.24, 2.42, 2.46, 2.27 and 2.37, while in every case the polydispersities of the adequately resolved bimodal distributions are 2 within experimental error for each peak.

The active site type present at 71°C is clearly stable, experiencing negligible deactivation over the polymerization times used (60 min) (see *Figure 4*). Its formation rate is also rapid, as no rate acceleration period was observed for the polymerization rates at 71°C. This suggests that perhaps site type I is a precursor to site type II. At 71°C, the formation rate of site type I is rapid; however, its transformation into site type II occurs slowly, if at all. As a consequence, virtually all of the polymer over the run period (60 min) is produced by site type I, and the polydispersity of this polymer is 2.

Table 2 Molecular weight data[a,b]

Run	T (°C)	$[Zr]_0$ (mmol l^{-1})	M_n	M_w/M_n
R-24	71	13.08×10^{-3}	24 000	2.05
R-18	50	13.08×10^{-3}	57 700	3.24
R-22	71	6.54×10^{-3}	32 000	1.96
R-19	50	6.54×10^{-3}	99 700	2.42
R-23	71	13.08×10^{-3}	21 600	1.97
R-20	50	13.08×10^{-3}	68 800	2.46
R-21	71	6.54×10^{-3}	29 300	1.97
R-17	50	6.54×10^{-3}	106 200	2.27
R-17	50	6.54×10^{-3}	106 00	2.37
R-15-R1	50	6.54×10^{-3}	132 100	1.85[c]
			2 700	1.77[d]
R-15-R2	50	6.54×10^{-3}	145 700	1.89[c]
			2 500	1.76[d]
R-15-R4	50	6.54×10^{-3}	141 400	1.95[c]
			2 600	1.80[d]

[a] Conditions for $[Al]_0$ are as in *Table 1*
[b] Coefficient of variation for $M_n = 5.0\%$, coefficient of variation for $M_w = 6.9\%$
[c] The molecular weight distributions of these samples are bimodal and the reported M_n and M_w values are for the high molecular weight peak
[d] The molecular weight distributions of these samples are bimodal and the reported M_n and M_w values are for the low molecular weight peak

It is clear that two active site types are present and there are at least two mechanisms by which these site types can be produced. One mechanism for producing the active site types is through the almost instantaneous production of one site type with the higher chain transfer/propagation rate constant ratio via reaction of MAO and Cp_2ZrCl_2, followed by a more gradual conversion of this site type to the site type with the lower chain transfer/propagation rate constant ratio. The other mechanism is via the instantaneous formation of two active site types with different propagation and chain transfer rate constants when MAO and Cp_2ZrCl_2 react, followed by the gradual conversion of the site type with the lower chain transfer/propagation rate constant ratio to the site type with the higher chain transfer/propagation rate constant ratio.

The variation in molecular weight with aluminium concentration is negligible (no changes observed within experimental error). Therefore, chain transfer to aluminium is not likely and hence will not be considered in the polymerization modelling which is to follow. The linear relationship between the inverse of the degree of polymerization and the inverse of the monomer concentration reported by Chien and Wang[8] confirms the importance of β-hydride chain transfer. This reaction is considered in the modelling study as the principal dead polymer formation reaction.

Model development

The underlying assumptions made in the development of the model are: (i) instantaneous formation of sites of the type that produces low molecular weight polymer at 50°C; (ii) transition of these sites to sites of the type that produce high molecular weight polymer at 50°C; (iii) first-order propagation with monomer and active sites as generally believed; (iv) β-hydride chain transfer; and (v) first-order deactivation of the sites that produce high molecular weight polymer. Bimolecular deactivation in the polymer phase is difficult to justify and is therefore not considered.

An irreversible first-order reaction with a pseudo-first-order rate constant was assumed for the transition reaction from site type I to site type II. This assumption will be discussed later using a correlation between the estimated pseudo-first-order rate constant and the operating variables.

With these assumptions, the polymerization reactions can be described as follows:

$$Zr + MAO \longrightarrow C_1^* \quad \text{instantaneous formation of } C_1^* \quad (1)$$

$$C_1^* + M \longrightarrow P_{1,1} \quad \text{instantaneous initiation of } C_1^* \quad (2)$$

$$P_{r,1} + M \xrightarrow{k_{p1}} P_{r+1,1} \quad \text{propagation of active species of type I} \quad (3)$$

$$P_{r,1} \xrightarrow{k_c} P_{r,2} \quad \text{transition reaction} \quad (4)$$

$$P_{r,2} + M \xrightarrow{k_{p2}} P_{r+1,2} \quad \text{propagation of active species of type II} \quad (5)$$

$$P_{r,1} + M \xrightarrow{k^*_{trm1}} Q_{r,1} + P_{1,1} \quad \text{transfer to monomer active species type I} \quad (6)$$

$$P_{r,2} + M \xrightarrow{k^*_{trm2}} Q_{r,2} + P_{1,2} \quad \text{transfer to monomer active species type II} \quad (7)$$

$$P_{r,2} + M \xrightarrow{k_{d2}} Q_{r,2} \quad \text{deactivation of active species type II} \quad (8)$$

where the ks, M, Q_r and P_r are, respectively, the rate constants, the monomer, dead polymer and living polymer. The asterisks in k^*_{trm1} and k^*_{trm2} indicate pseudo rate constants which also account for β-hydride chain transfer. $P_{r,1}$ is the polymer with chain length 'r' on site type I, which produces low molecular weight polymer at 50°C, and $P_{r,2}$ is the polymer with the same chain length 'r' but on site type II, which produces high molecular weight polymer at 50°C. $Q_{r,1}$ and $Q_{r,2}$ are, respectively, the polymers produced from deactivation and chain transfer. Then the model equations for a semi-batch reactor may be written accordingly

$$\frac{dM}{dt} = -k'_{trm1}P_{eth}L'_{0,1} - k'_{trm2}P_{eth}L'_{0,2} - k'_{p1}P_{eth}L'_{0,1} - k'_{p2}P_{eth}L_{0,2} + \frac{F_{i_{eth}}}{V_{rm}} \quad (9)$$

The first two terms of the right-hand side of equation (9) are negligible, as is the consumption of M in equation (2) for initiation. The following equation is obtained when equation (9) is multiplied by V_{rm}, which is the volume of the reaction mixture

$$\frac{dM}{dt} = -k'_{p1}P_{eth}L_{0,1} - k'_{p2}P_{eth}L_{0,2} + F_{i_{eth}} \quad (10)$$

The close agreement (6.9%) between the polymer yield determined by gravimetry and the polymer yield estimated from ethylene inflow ($F_{i_{eth}}$) measurements obtained with the mass flowmeter indicates that the total number of moles of ethylene (M) in the reaction mixture is nearly constant with time ($dM/dt \approx 0$), and that the flowmeter accurately measures the ethylene consumption rate (mol min^{-1}). Both sides of the following equations were also multiplied by V_{rm}

$$\frac{dP_{1,1}}{dt} = -k_cP_{1,1} - k'_{p1}P_{eth}P_{1,1} + k'_{trm1}P_{eth}L_{0,1} - k'_{trm1}P_{eth}P_{1,1} \quad (11)$$

$$\frac{dP_{1,2}}{dt} = k_cP_{1,1} - k_{p2}P_{eth}P_{1,2} - k_{d2}P_{1,2} + k'_{trm2}P_{eth}L_{0,2} - k'_{trm2}P_{eth}P_{1,2} \quad (12)$$

$$\frac{dP_{r,1}}{dt} = -k_cP_{r,1} - k'_{p1}P_{eth}P_{r,1} + k'_{p1}P_{eth}P_{r-1,1} - k'_{trm1}P_{eth}P_{r,1} \qquad r>1 \quad (13)$$

$$\frac{dP_{r,2}}{dt} = k_cP_{r,1} - k'_{p2}P_{eth}P_{r,2} + k'_{p2}P_{eth}P_{r-1,2} - k'_{trm2}P_{eth}P_{r,2} - k_{d2}P_{r,2} \quad r>1 \quad (14)$$

$$\frac{dQ_{r,1}}{dt} = k'_{trm1}P_{eth}P_{r,1} \quad (15)$$

$$\frac{dQ_{r,2}}{dt} = k'_{trm2}P_{eth}P_{r,2} + k_{d2}P_{r,2} \quad (16)$$

where the k's are the products of the ks and k_{eq}. $L_{n,1}$ and $L_{n,2}$ are the moments of nth order for propagating

polymer on site types I and II, respectively, defined as

$$L_{n,1}=\Sigma r^n P_{r,1} \qquad L_{n,2}=\Sigma r^n P_{r,2} \tag{17}$$

The moments of nth order for dead polymer are defined as

$$J_{n,1}=\Sigma r^n Q_{r,1} \qquad J_{n,2}=\Sigma r^n Q_{r,2} \tag{18}$$

The initial ($t=0$) conditions can therefore be summarized as follows

$$M=k_{eq}P_{eth}$$

$$P_{r,1}=P_{r,2}=L_{n,2}=0 \text{ (with } r>2 \text{ for site type I and } r>1 \text{ for site type II)}$$

$$Q_{r,1}=Q_{r,2}=J_{n,1}=J_{n,2}=0 \text{ (with } r>1)$$

$$P_{1,1}=L_{n,1}=N^*_{10}$$

where N^*_{10} is the initial molar mass of the active species of type I in the reactor. In formulating equations (9) to (16) we assume: (i) that the polymer phase is in equilibrium with the gas phase; and (ii) that diffusional effects within the polymer phase are negligible.

Multiplying equations (11) to (16) by r^0, r^1, and r^2 and summing over all values of r gives the following moment equations after application of the long chain approximation (LCA)

$$\frac{dL_{0,1}}{dt}=-k_c L_0 \tag{19}$$

$$\frac{dL_{1,1}}{dt}=(k'_{p1}P_{eth}+k'_{trm1}P_{eth})L_{0,1}-(k_c+k'_{trm1}P_{eth})L_{1,1} \tag{20}$$

$$\frac{dL_{2,1}}{dt}=2k'_{p1}P_{eth}L_{1,1}+(k'_{p1}P_{eth}+k'_{trm1}P_{eth})L_{0,1}-(k'_{trm1}P_{eth}+k_c)L_{2,1} \tag{21}$$

$$\frac{dJ_{0,1}}{dt}=k'_{trm1}P_{eth}L_{0,1} \tag{22}$$

$$\frac{dJ_{1,1}}{dt}=k'_{trm1}P_{eth}L_{1,1} \tag{23}$$

$$\frac{dJ_{2,1}}{dt}=k'_{trm1}P_{eth}L_{2,1} \tag{24}$$

$$\frac{dL_{0,2}}{dt}=k_c L_{0,1}-k_{d2}L_{0,2} \tag{25}$$

$$\frac{dL_{1,2}}{dt}=k_c L_{1,1}+(k'_{p2}P_{eth}+k'_{trm2}P_{eth})L_{0,2}-(k_{d2}+k'_{trm2}P_{eth})L_{1,2} \tag{26}$$

$$\frac{dL_{2,2}}{dt}=k_c L_{2,1}+2k'_{p2}P_{eth}L_{1,2}+(k'_{p2}P_{eth}+k'_{trm2}P_{eth})L_{0,2}-(k_{d2}+k'_{trm2}P_{eth})L_{2,2} \tag{27}$$

$$\frac{dJ_{0,2}}{dt}=(k_{d2}+k'_{trm2}P_{eth})L_{0,2} \tag{28}$$

$$\frac{dJ_{1,2}}{dt}=(k_{d2}+k'_{trm2}P_{eth})L_{1,2} \tag{29}$$

$$\frac{dJ_{2,2}}{dt}=(k_{d2}+k'_{trm2}P_{eth})L_{2,2} \tag{30}$$

Equations (10), (19) and (25) can be solved separately to give the polymerization rate model

$$\text{rate}=[k'_{p1}N^*_{10}e^{-k_c t}+\frac{k_c k'_{p2}N^*_{10}}{k_c-k_{d2}}(e^{-k_{d2}t}-e^{-k_c t})]P_{eth} \tag{31}$$

Defining the lumped parameters

$$\theta_1=k'_{p1}N^*_{10}$$

$$\theta_2=k'_{p2}N^*_{10}$$

transforms equation (31) to

$$\text{rate}=[\theta_1 e^{-k_c t}+\frac{k_c\theta_2}{k_c-k_{d2}}(e^{-k_{d2}t}-e^{-k_c t})]P_{eth} \tag{32}$$

Equations (19) to (30) were integrated numerically to obtain the zero, first and second moments of L and J. The number average and weight average molecular weights of the polymer produced by each site type can then be calculated from

$$M_{n1}=\frac{L_{1,1}+J_{1,1}}{L_{0,1}+J_{0,1}}M_m \qquad M_{w1}=\frac{L_{2,1}+J_{2,1}}{L_{1,1}+J_{1,1}}M_m \tag{33}$$

$$M_{n2}=\frac{L_{1,2}+J_{1,2}}{L_{0,2}+J_{0,2}}M_m \qquad M_{w2}=\frac{L_{2,2}+J_{2,2}}{L_{1,2}+J_{1,2}}M_m \tag{34}$$

and the number average and weight average molecular weights of the whole polymer can be calculated from

$$M_n=\frac{L_{1,1}+J_{1,1}+L_{1,2}+J_{1,2}}{L_{0,1}+J_{0,1}+L_{0,2}+J_{0,2}}M_m$$

$$M_w=\frac{L_{2,1}+J_{2,1}+L_{2,2}+J_{2,2}}{L_{1,1}+J_{1,1}+L_{1,2}+J_{1,2}}M_m \tag{35}$$

where M_m is the molecular weight of the monomer.

Parameter estimation

Parameters θ_1, θ_2, k_c and k_{d2} were estimated by fitting the polymerization rate model given in equation (32) to each experimental run in the design shown in *Table 1*. Empirical relationships were then developed between these estimates and the operating conditions for MAO batch 2. A conversion factor was employed in order to give measured and fitted polymerization rates with the same units (mol min^{-1}).

An ordinary least-squares analysis was employed to fit equation (32) to the measured polymerization data for each run. For those operating conditions under which replicate runs were conducted, all the replicates were lumped together to estimate the parameters for that particular set of operating conditions. The parameter estimates obtained for equation (32) are shown in *Table 3*.

Table 4 shows an excellent agreement between the experimental and predicted M_n and M_w values. Before the average molecular weights were calculated, values for the parameters of equation (32), where the polymerization rate model was fitted to the data, were substituted in equations (19) to (30). Values for N^*_{10}, k'_{trm1} and k'_{trm2} were assigned until the agreement shown in *Table 4* was achieved. The values shown in *Table 5* are under no circumstances statistical estimates. If one uses the model with values of N^*_{10} higher than those reported in *Table 5* for runs at 50°C, the agreement between the

Table 3 Parameter estimates for polymerization rate model equation (32) for the eight sets of operating conditions using MAO batch 2[a]

Run	θ_1 (mol min^{-1} psi^{-1})	θ_2 (mol min^{-1} psi^{-1})	k_c (min^{-1})	k_{d2} (min^{-1})
R-24-R2	0.000788	0.00179	0.00591	0.0357
	(0.0000385)	(0.00248)	(0.0182)	(0.178)
R-18-R1	0.000548	0.000953	2.842	0.0366
	(0.000216)	(0.000031)	(2.093)	(0.00193)
R-22-R1	0.000890	0.00222	0.00403	0.2569
	(0.0000578)	(0.0110)	(0.00109)	(1.107)
R-19-R1	0.000302	0.000830	0.369	0.0218
	(0.000073)	(0.0000343)	(0.112)	(0.00191)
R-23-R1	0.000865	0.000784	0.00666	0.0269
	(0.0000377)	(0.000735)	(0.0367)	(0.277)
R-20-R1	0.000626	0.00105	0.0619	0.0530
	(0.0000453)	(0.000885)	(0.00473)	(0.115)
R-21-R1	0.000817	0.000515	0.00474	0.0339
	(0.0000379)	(0.000845)	(0.0237)	(0.495)
R-17-R2, -R3	0.000324	0.000802	0.250	0.0228
	(0.0000431)	(0.0000113)	(0.0540)	(0.00175)

[a] The values in parentheses are the standard deviation associated with the corresponding estimates

Table 4 Fitted and experimental molecular weights of polyethylene with a unimodal distribution

	Experimental		Fitted	
Run	M_n	M_w	M_n	M_w
R-24-R2	24 000	49 200	25 300	50 600
R-18-R1	57 700	187 400	55 600	190 800
R-22-R1	32 000	63 000	31 300	62 600
R-19-R1	99 700	242 000	98 100	242 700
R-23-R1	21 600	42 600	21 400	42 800
R-20-R1	68 800	169 800	67 600	170 700
R-21-R1	29 300	58 000	29 200	58 400
R-17[a]	106 200	247 000	106 300	253 900

[a] Experimental M_n and M_w are the average values of the M_n and M_w measured for polymer samples obtained in replicate runs R-17, -R1 and -R2

Table 5 Parameter estimates for M_n and M_w models (equations (19) to (30)) for the eight sets of operating conditions using MAO batch 2[a]

Run	T (°C)	$10^6 N_{10}^*$ (mol)	k'_{trm1} (min^{-1} psi^{-1})	k'_{trm2} (min^{-1} psi^{-1})
R-24	71	13.080	0.065	[b]
R-18	50	10.060	1.340	0.022
R-22	71	6.540	0.120	[b]
R-19	50	3.200	0.215	0.0554
R-23	71	13.080	0.085	[b]
R-20	50	0.880	0.494	0.2980
R-21	71	6.540	0.118	[b]
R-17	50	1.860	0.220	0.0885

[a] Conditions for $[Zr]_0$ and $[Al]_0$ are as in *Table 1*
[b] The chain transfer rate constant cannot be estimated since the amount of polymer produced by active centres of type II is negligible

experimental and model molecular weights of the whole polymer will still be close but the polydispersity of one of the two peaks becomes less than 2. However, the model with values of N_{10}^* equal to the initial numbers of moles of zirconium $[Zr]_0$ (which are the highest values that one can assign to N_{10}^*) will give good results for the M_n and M_w of the whole polymer for runs at 71°C.

Table 6 Propagation rate constants of both types of active species for the eight sets of operating conditions using MAO batch 2[a]

Run	T (°C)	$10^6 N_{10}^*$ (mol)	k'_{p1} (min^{-1} psi^{-1})	k'_{p2} (min^{-1} psi^{-1})
R-24	71	13.080	60.2	[b]
R-18	50	10.060	54.4	94.7
R-22	71	6.540	136.0	[b]
R-19	50	3.200	94.3	259.3
R-23	71	13.080	66.1	[b]
R-20	50	0.880	711.3	1193.1
R-21	71	6.540	124.9	[b]
R-17	50	1.860	174.1	431.1

[a] Conditions for $[Zr]_0$ and $[Al]_0$ are as in *Table 1*
[b] The chain transfer rate constant cannot be estimated since the amount of polymer produced by active centres of type II is negligible

The values of N_{10}^* shown in *Table 5* were used to obtain the k'_{p1} and k'_{p2} values shown in *Table 6*. For solving equations (19) to (30) a routine called LSODAR, developed at Sandia National Laboratories and Lawrence Livermore National Laboratory[11,12], was employed. This routine solves ordinary differential equations with automatic method switching for stiff and non-stiff problems.

In order to test the adequacy of a fitted model and calculate the precision of its estimated parameter, it is necessary to know the pure error variance. The pure error variance of the polymerization rate data (359.8) was estimated from replicate set R-15, which includes the dry solvent batch as one source of experimental error between runs.

The adequacy of the model was assessed using an F test and residuals plots from the fitted model[13]. The fitted model, i.e. equation (32), was found adequate for each of the eight sets of operating conditions. From these results and the small differences obtained between the experimental and fitted average molecular weights, it can be concluded that the proposed model provides an adequate representation of the data in the experimental region studied. For illustration, *Figure 6* shows a

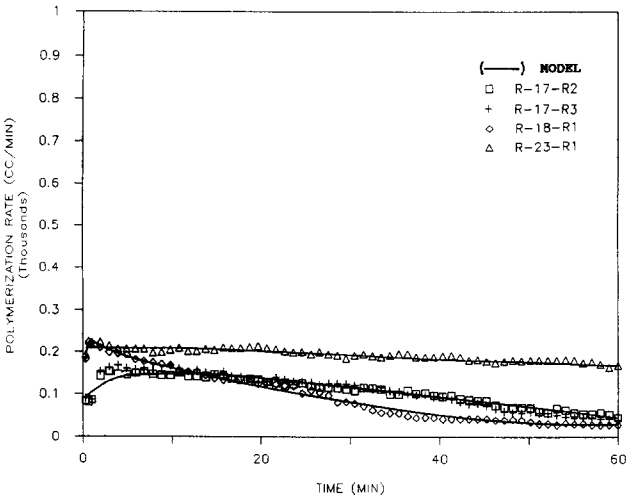

Figure 6 Kinetic rate curves (model predictions and experimental data) using MAO batch 2 at $T=50°C$ (R-17) and 71°C (R-18, R-23). The operating conditions for $[Zr]_0$ and $[Al]_0$ can be found in *Table 1*

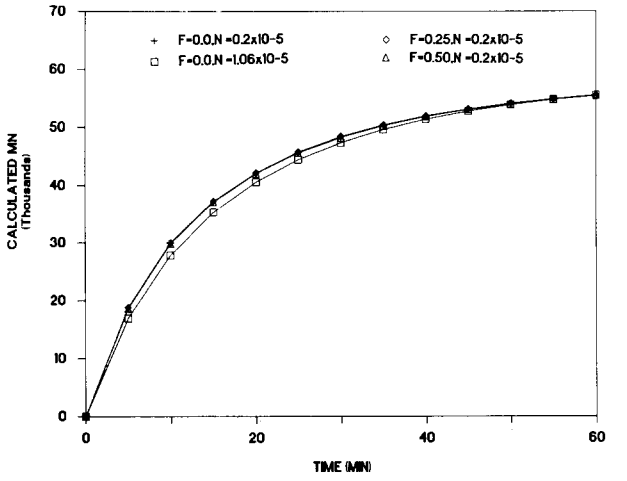

Figure 7 Comparison of M_n values for the two models involving two site types based on different mechanisms. When $F=0$ (defined as the ratio of the initial number of active centres of type II (N^*_{20} to the initial number of active centres of type I N^*_{10}), M_n is calculated with equations (19) to (30), which accounts for the initial, instantaneous formation of one site type. When $F=0.25$ and 0.5, M_n is calculated with a model which accounts for the instantaneous formation of two site types at time zero

comparison of the experimental and fitted polymerization rates for runs R-17-R2, R-17-R3, R-18-R1, and R-23-R1.

The polymerization rate model based on the second mechanism (i.e. the instantaneous formation of two active site types and then the gradual conversion of the site type with the higher chain transfer/propagation rate constant ratio to the site type with the lower chain transfer/propagation rate constant ratio) becomes equation (32) with θ_1 defined as $k'_{p1}N^*_{10}+k'_{p2}N^*_{20}$ (N^*_{10} and N^*_{20} are the initial molar masses of site types I and II, respectively). *Figures 7* and *8*, respectively, show M_n and M_w values for both mechanisms. When $F=0$, defined as N^*_{20}/N^*_{10}, M_n and M_w are calculated with equations (19) to (30). It is evident that the M_n and M_w values calculated with the second model ($F>0$) can also be obtained with the first model (equations (19) to (30)) by adjusting N^*_{10}. This means that one model cannot be discriminated from the other using polymerization rate and average molecular weight data. However, for the purpose of providing an acceptable kinetic model, the model described above appears reasonable even though it may be superseded by another model when additional experimental data become available.

RESULTS AND DISCUSSION

Since exact knowledge of the functional relationships between the kinetic parameters and operating variables was not available, we developed the functions empirically using first-order relationships. From a regression analysis, retaining only significant terms, we obtained the following relationship for the $k'_{p1}N^*_{10}/k'_{p2}N^*_{10}$ ratio, for which no model inadequacy was found

$$10\ln\left(\frac{k'_{p1}N^*_{10}}{k'_{p2}N^*_{10}}\right)=-4.70-2.49[Al]'_0+1.25[Zr]'_0+2.80T'+1.17[Al]'_0[Zr]'_0-2.19[Al]'_0T'-0.87[Zr]'_0T'+1.02[Al]'_0[Zr]'_0T' \quad (36)$$

where the prime (') denotes a coded value of the operating variable defined by

$$\text{coded variable}=\frac{\text{measured value}-(\text{upper limit}+\text{lower limit})/2}{(\text{upper limit}-\text{lower limit})/2}$$

where the values of the lower and upper limits of each operating variable can be found in *Table 1*. The coefficients reflect the individual effects of the corresponding operating variables and their interaction effects with other operating variables.

This result is somewhat surprising since we expected that the temperature would be the only important variable. However, this relationship shows that the activity of each active site type is greatly affected by all three operating variables, and the importance of the interaction effects suggests that a complex activation process is occurring. Chien and Wang[8] proposed that

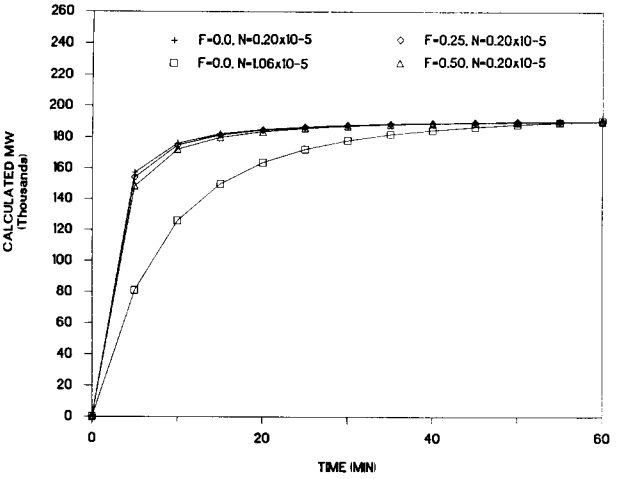

Figure 8 Comparison of M_w values for the two models involving two site types based on different mechanisms. When $F=0$ (defined as the ratio of the initial number of active centres of type II (N^*_{20} to the initial number of active centres of type I N^*_{10}), M_w is calculated with equations (19) to (30), which accounts for the initial, instantaneous formation of one site type. When $F=0.25$ and 0.5, M_w is calculated with a model which accounts for the instantaneous formation of two site types at time zero

the transition metal of the two active site types, neutral and cationic, could be coordinated to zero, one or two MAOs, resulting in active centres of different k_p. It seems that the number of coordinated MAOs depends on the polymerization operating conditions. Sinn *et al.*[14] have proposed that the zirconium compound diffuses into an association of methylaluminoxanes to form the catalytic centre. The zirconium diffusion rate certainly would depend on temperature and the number of methylaluminoxane molecules associated.

The relationship between k_c and the operating variables was obtained in a similar fashion as follows

$$10 \ln k_c = -31.39 - 21.11T' \quad (37)$$

As mentioned earlier, k_c is a pseudo-first-order rate constant. Actually, the negative effect of temperature on k_c indicates that the transition reaction is not elementary. It is reasonable to say that a reversible reaction is likely, and equation (37) supports it. If the activation energy of the reaction of sites of type II (species 2) to produce sites of type I (species 1) is higher than the activation energy of the reaction of species 1 to produce species 2, the rate constant of the former reaction will be more sensitive to an increase in temperature. Hence, when the temperature is increased the production of species 2 is drastically decreased. *Figure 9* shows the effect of an increase in the reaction rate of species 2 to produce species 1 on the predicted polydispersity. It can be clearly observed that the polydispersity tends to 2 (indicating the presence of one site type) as the rate of formation of species 1 from species 2 becomes predominant ($k_1/k_2 > 10$). The dissociation equilibrium of the less active ligated species (species 1) to a more active species with a different MAO ligation or none (species 2) may be present at 71°C since a rate acceleration period was not observed. The analysis of equation (37) also suggests that the longer rate acceleration period observed at the lower zirconium concentration is likely due to the slower transition of species 1 to species 2.

As expected, the precision of the estimates of k_{d2} for 71°C is poor as large standard deviations for runs R-21, R-22, R-23, and R-24 in *Table 4* can be observed. Most important is the fact that the differences between the k_{d2} values estimated at 50°C and the k_{d2} values estimated at 71°C are much smaller than the aforementioned standard deviations. Hence the following relationship for k_{d2} was obtained for runs at 50°C

$$10 \ln k_{d2} = -34.61 \quad (38)$$

Interestingly, k_{d2} is independent of the operating variables ($[Al]_0$ and $[Zr]_0$). This suggests that the effects of the aluminium and zirconium concentrations on the deactivation reaction are much more complicated than a linear correlation can represent. The deactivation reaction is often further complicated by the possible presence of unknown impurities.

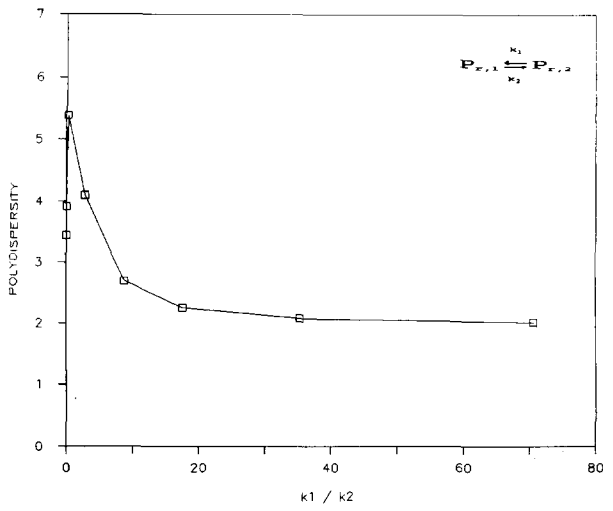

Figure 9 Effect of an increase in the rate of formation of active centres of type I from active centres of type II on polydispersity

Table 7 Model and experimental molecular weights of polyethylene with a bimodal distribution

	Experimental		Model	
Run	M_n	M_w	M_n	M_w
R-15-R1	132 100	244 400	122 700	244 000
	2 700	4 800	2 700	5 300
R-15-R2	145 700	276 400	139 000	276 600
	2 500	4 400	2 500	5 000
R-15-R4	141 400	276 200	138 900	276 400
	2 500	4 700	2 500	5 000

Table 8 Model-calculated molecular weights of polymer produced by each type of active centre[a,b]

Run	T (°C)	M_{n1}	M_{w1}	M_{n2}	M_{w2}
R-24	71	25 300	50 600	[c]	[c]
R-18	50	920	1 810	96 600	192 200
R-22	71	31 300	62 600	[c]	[c]
R-19	50	10 500	21 000	124 800	248 400
R-23	71	21 400	42 800	[c]	[c]
R-20	50	39 900	79 700	111 600	222 200
R-21	71	29 200	58 400	[c]	[c]
R-17	50	20 000	39 900	132 500	263 700

[a] Conditions for $[Zr]_0$ and $[Al]_0$ are as in *Table 1*
[b] The predicted average molecular weights of the whole polymer are shown in *Table 4*
[c] The amount of polymer produced by active centres of type II is negligible

Interestingly, k_{d2} is independent of the operating variables ($[Al]_0$ and $[Zr]_0$). This suggests that the effects of the aluminium and zirconium concentrations on the deactivation reaction are much more complicated than a linear correlation can represent. The deactivation reaction is often further complicated by the possible presence of unknown impurities.

The close agreements between the experimental and fitted M_n and M_w values shown in *Table 4* are an encouraging indication of the validity of a model involving two site types. More encouraging is the content of *Table 7*. The model calculates accurately the M_n and M_w values of both the high and low molecular weight peaks for polymer samples obtained with MAO batch 1. *Table 8* shows that the model is consistent in predicting the molecular weights for each type of active centre. Site type I produces the low molecular weight polymer ($M_w/M_n = 2$) and site type II produces the high molecular weight polymer ($M_w/M_n = 2$) for runs at 50°C. The model also predicts the average molecular weights of the whole polymers produced in runs at 71°C with only site type I.

More evidence of the validity of the model is the much higher ratio of k'_{trm1} to k'_{trm2} for run R-15 (24.0) than for run R-17 (2.4). It was mentioned above that a large difference between the chain transfer constant of site type I and the chain transfer constant of site type II was probably what caused the bimodal distribution of the polymer produced in R-15 (MAO batch 1), and if this difference becomes smaller the distribution becomes unimodal like the one obtained in run R-17 (MAO

batch 2). From *Table 5* one can calculate ratios of k'_{trm1} to k'_{trm2} lower than 24.0 for runs R-17, R-19 and R-20 (2.4, 3.8 and 1.6) and much higher than 24.0 for run R-18 (60.9). However, the distributions of these runs, including R-18, were unimodal. The high ratio for run R-18 indicates that the model may predict a bimodal distribution, particularly if k'_{p1} and k'_{p2} are very different. In fact *Table 8* shows that the calculated molecular weight for site type I is much smaller than the calculated molecular weight for site type II. However, it is important to point out that the poor precision of k_c (large standard deviation shown in *Table 3* for run R-18) makes difficult the selection of reasonable values for k'_{trm1} and k'_{trm2} to match the predicted and experimental molecular weights.

A qualitative assessment of the k'_p values shown in *Table 6* provides further evidence of the validity of the model. As expected for runs at 50°C (rate acceleration period observed), the apparent propagation rate constants for active centres of type I (k'_{p1}) are smaller than the apparent propagation rate constants for active centres of type II (k'_{p2}). It is interesting to note (*Table 6*) that the initial number of active centres ($N^*_{1_0}$) is smaller than the initial number of moles of zirconium ($[Zr]_0$) at 50°C but equal to $[Zr]_0$ at 71°C, which means that the catalyst efficiency ($N^*_{1_0}/[Zr]_0$) increases with temperature and may be 100% before the temperature reaches 71°C. Chien and Wang[8] reported an efficiency of 100% (determined by radiolabelling) for polymerizations carried out at 70°C with $[Zr]_0 = 3.8 \times 10^{-3}$ mmol l^{-1}. The high level of $[Zr]_0$ (13.08×10^{-3} mmol l^{-1}) in our experimental design is 3.7 times lower than the level of zirconium at which they found an efficiency less than 100% (84%).

Table 2 shows that the molecular weight decreases significantly with increasing temperature. This can be explained by the high k'_p/k'_{trm} ratios for the active centres of type II (shown in *Table 9*), which are dominant at 50°C, and the low k'_p/k'_{trm} ratios for the active centres of type I (shown in *Table 9*), which are practically the only type of active centre present at 71°C.

Table 2 also shows the effect of the concentration of zirconium compound on molecular weight. This effect is negative and much larger at 50°C than at 71°C. The change in sensitivity of molecular weight to zirconium can be explained by the importance of the chain transfer reaction at a particular temperature. At 71°C the chain transfer reaction must be faster (species 1 with large k_{trm1} are the only active species present) than the chain transfer reaction at 50°C (species 2 with small k_{trm2} constitute most of the active centres). Therefore, the higher k'_p/k'_{trm} ratios for active centres of type II (*Table 9*) come from the contributions of higher k_p and lower k_{trm}. Surprisingly, the apparent chain transfer rate constant (k'_{trm}, defined by the product of an equilibrium constant and the chain transfer rate constant k_{trm}) at 50°C is larger than the apparent chain transfer rate constant at 71°C (see *Table 5*). This is because the negative effect of temperature on the equilibrium partition of monomer between the gaseous and polymer phases is larger than the positive effect of temperature on k_{trm}.

An interesting implication of the model is shown in *Figure 10*. For $k_c = 0$ the polydispersity is 1 as $k'_{trm1} \to 0$, indicating that living polymerization is taking place. Equation (37) and *Table 5* show that as the temperature increases, $k_c \to 0$ and k'_{trm1} decreases. However, $k'_{trm1} = 0$ only if the equilibrium monomer partition constant is 0, which means no monomer is held in the liquid phase. This suggests that living polymerization will not take place with this catalytic system.

Table 9 The k'_p/k'_{trm} ratios for the eight sets of operating conditions using MAO batch 2[a]

Run	T (°C)	$10^6 N^*_{1_0}$ (mol)	k'_{p1}/k'_{trm1}	k'_{p2}/k'_{trm2}
R-24	71	1.160	926.1	[b]
R-18	50	0.650	40.5	4304.5
R-22	71	1.050	1133.3	[b]
R-19	50	0.154	438.6	4680.5
R-23	71	1.500	777.6	[b]
R-20	50	0.160	1439.8	4003.6
R-21	71	1.050	1058.4	[b]
R-17	50	0.142	791.3	4871.1

[a] Conditions for $[Ar]_0$ and $[Al]_0$ are as in *Table 1*
[b] The chain transfer rate constant cannot be estimated since the amount of polymer produced by active centres of type II is negligible

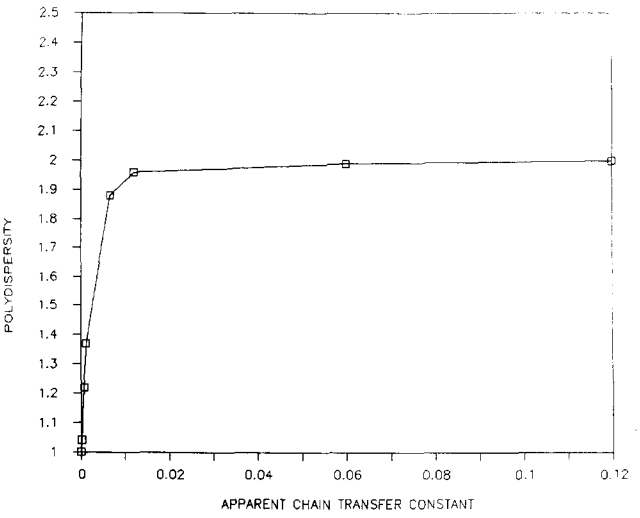

Figure 10 Effect of chain transfer on polydispersity

CONCLUSIONS

A kinetic model has been developed for the polymerization of ethylene with Cp_2ZrCl_2/MAO as catalyst, based on polymerization rate and molecular weight data. The data with kinetic modelling suggest that two active centre types are present. One kind of species undergoes instantaneous initiation followed by first-order propagation with monomer, β-hydride chain transfer and pseudo-first-order transformation to the other kind of active species. The second type of active species experiences first-order propagation with monomer, chain transfer to monomer and first-order deactivation of the polymerization rate from a value reached within the first three minutes of reaction, the polydispersities higher than 2 with bimodal distributions sometimes forming, or the reduction of catalyst deactivation rate at a higher temperature.

The experimental effort was minimized effectively with the use of experimental design techniques. A statistical analysis was applied to the information obtained in this investigation.

In our experiments ethylene concentrations were constant and therefore it was not possible to differentiate between chain transfer to monomer and β-hydride chain transfer.

ACKNOWLEDGEMENT

We are grateful to G. N. Foster (Union Carbide) for performing the g.p.c. measurements.

REFERENCES

1 Weissermel, K., Cherdron, H., Berthold, J., Diedrich, B., Keil, K. D., Rust, K., Strametz, H. and Toth, T. *J. Polym. Sci., Polym. Symp. Edn* 1975, **51**, 187
2 Chien, J. C. W. and Wang, B. P. *J. Polym. Sci., Polym. Chem. Edn* 1988, **26**, 3089
3 Kaminsky, W. in 'Transition Metal Catalyzed Polymerization' (Ed. R. P. Quirk), Vol. 4, MMI Press, London, 1983, p. 225
4 Kaminsky, W., Bark, A., Speihl, R., Moller-Lindenhof, N. and Niedoba, S. in 'Transition Metals and Organometallics as Catalysts for Olefin Polymerization' (Eds W. Kaminsky and H. Sinn), Springer-Verlag, Berlin, 1988, p. 291
5 Kaminsky, W. in 'Catalytic Polymerization of Olefins' (Eds T. Keii and K. Soga), Kodansha, Tokyo, 1986, p. 293
6 Kaminsky, W. and Schlobohm, M. *Makromol. Chem., Macromol. Symp.* 1986, **4**, 103
7 Schmidt, G. F. in 'Transition Metal Catalyzed Polymerization' (Ed. R. P. Quirk), Cambridge University Press, Cambridge, 1988, p. 151
8 Chien, J. C. W. and Wang, B. P. *J. Polym. Sci., Polym. Chem. Edn* 1990, **28**, 15
9 Kaminsky, W. and Hahnsen, H. *US Pat. 4455762*, 1985
10 Reichert, K. H. in 'Transition Metal Catalyzed Polymerization' (Ed. R. P. Quirk), Vol. 4, MMI Press, London, 1983, p. 465
11 Hindmarsh, A. C. *ACM-SIGNUM Newslett.* 1980, **15**, 10
12 Petzold, L. R. Sandia National Laboratories, Report SAN80-8230, Livermore, 1980
13 Draper, N. R. and Smith, H. 'Applied Regression Analysis,', Wiley, New York, 1980, p. 62
14 Sinn, H., Kaminsky, W., Vollmer, H. J. and Woldt, R. *Angew. Chem., Int. Edn Engl.* 1980, **19**, 390